



ELSEVIER

Journal of Alloys and Compounds 293–295 (1999) 838–843

Journal of  
ALLOYS  
AND COMPOUNDS

# Hydrogen transport between proton conducting oxide and hydrogen storage metal

S. Horiike, A. Kunimatsu, K. Takahiro, S. Nagata, S. Yamaguchi\*

*Institute for Materials Research, Tohoku University, Sendai 980-8577, Japan*

## Abstract

We constructed an electrochemical cell consisting of proton conducting oxide as an electrolyte and hydrogen storage metal as a negative electrode. Hydrogen transport between the proton conducting oxide and the hydrogen storage metal, which is induced by the gradient of electric potential or the hydrogen concentration, was studied by the measurements of electromotive force (EMF) and proton flux across the electrolyte. The transport of protons from  $\text{SrCe}_{0.95}\text{Yb}_{0.05}\text{O}_{3-\alpha}$  proton conducting oxide to the hydrogen storage metals of V and Zr induced by the electric potential was investigated from the measurement of proton flux which flows in the negative electrode, where the proton flux was determined from the time evolution of the hydrogen content in the electrode material which could be obtained by the d.c. current and the ERDA measurements. From the relations between the hydrogen flux and the total electric current across the electrolyte, we evaluated the proton transport numbers and the proton diffusivity for  $\text{SrCe}_{0.95}\text{Yb}_{0.05}\text{O}_{3-\alpha}$  oxide used as the electrolyte. As for the hydrogen transport from the hydrogen storage metal to the proton conducting oxide, we observed the temporal evolution of the voltage between the electrodes. The temperature dependence of the electromotive force revealed that the protons emitted from the hydrogen storage metals such as V, Zr, Nb and  $\text{LaNi}_5$  had entered into the proton conducting oxide. This result indicated that the hydrogen storage metals have a possibility to be used as the negative hydrogen electrode of the hydrogen–air fuel cell. © 1999 Elsevier Science S.A. All rights reserved.

**Keywords:** Electrochemical cell; Proton conducting oxide electrolyte; Hydrogen storage metal

## 1. Introduction

The study and the development of hydrogen–air fuel cells are interesting and promising for the power generation system without the drain of fuel and the ecological problems. On the basis of experimental results and theoretical evaluations we believe that the realization of new types of fuel cells characterized by using hydride electrodes and a solid electrolyte is technically feasible. Proton conducting oxides such as  $\text{SrCe}_{0.95}\text{Yb}_{0.05}\text{O}_{3-\alpha}$  and  $\text{BaCe}_{0.9}\text{Y}_{0.1}\text{O}_{3-\alpha}$  have a large potential for use as a solid electrolyte in electrochemical processes such as fuel cell and steam electrolysis [1]. As for the hydrogen storage metal, utilization as a hydrogen electrode in the hydrogen–air fuel cells as well as a hydrogen storage media in the steam electrolyzer is realized [2,3]. In order to improve the hydrogen–air fuel cell consisting of the proton conducting oxides as the solid electrolyte and the hydrogen storage metals as the hydrogen electrode, knowledge about the

electrochemical reactions between the electrolyte and the electrode, especially the hydrogen (proton) transport between the proton conducting oxides and hydrogen storage metals, will be indispensable.

Hydrogen transport between the proton conducting oxide and the hydrogen storage metal which is induced by electric field or hydrogen (proton) concentration gradient can be examined by the Elastic Recoil Detection Analysis (ERDA) technique using a high-energy  $^4\text{He}$  ion beam as shown in our previous work [4,5]. It was found that protons dissolved in  $\text{SrCe}_{0.95}\text{Yb}_{0.05}\text{O}_{3-\alpha}$  migrated towards the negative electrode driven by the electric potential, and they were trapped there when the electrode material had a good ability to collect the migrating hydrogen. The amount of hydrogen accumulated in the electrode was measured by the ERDA method.

In the present work, we construct the electrochemical cell in which the proton conducting oxide and the hydrogen storage metal are used as the solid electrolyte and the negative electrode, respectively.  $\text{SrCe}_{0.95}\text{Yb}_{0.05}\text{O}_{3-\alpha}$  oxide is chosen as the electrolyte because of its high ionic conductivity. The hydrogen storage metals of V, Zr, Nb and  $\text{LaNi}_5$  are used as the negative hydrogen electrodes. In

\*Corresponding author. Tel.: +81-222-152-060; fax: +81-222-152-061.

E-mail address: yoshida@wani.imr.tohoku.ac.jp (S. Yamaguchi)

this electrochemical cells, we investigate the hydrogen transport from the proton conducting oxide to the hydrogen storage metal, and determine the proton transport number and the proton diffusivity. Also, we observe the temporal evolution of the voltage caused by the proton concentration gradient to examine the hydrogen transport from the hydrogen storage metal to the proton conducting oxide.

## 2. Experimental

The electrochemical cell used in the present work is illustrated schematically in Fig. 1. The mixture of water vapor and nitrogen gases or the mixture of oxygen and nitrogen gases was supplied to the positive compartment, while the negative component was sealed tightly to prevent the release of hydrogen. The partial pressure of water vapor was controlled by changing temperature of water which was saturated with water vapor. A disc-shaped polycrystalline pellet of  $\text{SrCe}_{0.95}\text{Yb}_{0.05}\text{O}_{3-\alpha}$  with 15 mm diameter and 0.5–1.0 mm thickness ( $\alpha$  is the number of oxygen deficiencies per perovskite-type oxide unit cell) was used as the electrolyte. The oxide pellet was prepared by a solid state reaction and sintering process using appropriate oxides and carbonates as starting materials. As a negative electrode material, the hydrogen storage metal film of about 200 nm thickness was evaporated on the one side surface of the disc-shaped pellet. The black-Pt coated Pt net attached to the other side surface of the pellet was used as a positive electrode. D.c. voltages of 25–200 V were applied on the electrode and the d.c. current through the specimen was recorded in a personal computer. The ERDA measurements were carried out by using  $^4\text{He}$  beam of 3.6 MeV energy from a 1.7 MV tandem accelerator.

Analyzing  $^4\text{He}$  beam was collimated with apertures less than  $0.01^\circ$  and the beam spot was about 1 mm. The elastically recoiled particles were detected at an angle of  $30^\circ$  from the incident direction. For the measurement of the proton flux across the electrolyte, we used the apparatus described in the previous papers [4,5], in which the electrochemical cell was mounted on the sample holder of the scattering chamber connected to 1.7 MV tandem accelerator. The temporal evolution of cell EMF was measured in the range 50–400°C.

## 3. Results and discussion

Fig. 2 shows time dependence of d.c. current through the electrolyte during the steam electrolysis at 120°C under various applied voltages, where the partial pressure of water vapor is 355 Torr. The d.c. current through the specimen increased with increase of the temperature, and was almost constant independent of the duration time at 120°C.

In order to obtain direct evidence of the proton migration in the  $\text{SrCe}_{0.95}\text{Yb}_{0.05}\text{O}_{3-\alpha}$  electrolyte induced by the electric potential, the numbers of the hydrogen accumulated in the V electrode were measured by means of the ERDA technique after the steam electrolysis. Examples of the ERDA spectra taken from the V film used as the negative electrode are shown in Fig. 3, where the peak near 320 channel comes from the hydrogen dissolved in the V electrode. As seen from this figure, the intensity of hydrogen peak of the cathode side increased after the steam electrolysis. The number of hydrogen retained in the V film is proportional to area of the hydrogen peak in the ERDA spectrum. Consequently, the number of hydrogen

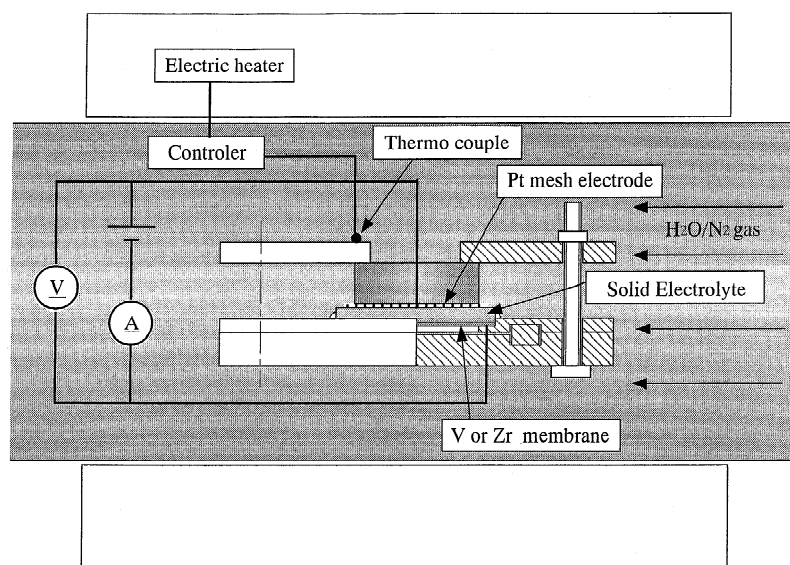


Fig. 1. Schematic illustration of electrochemical cell.

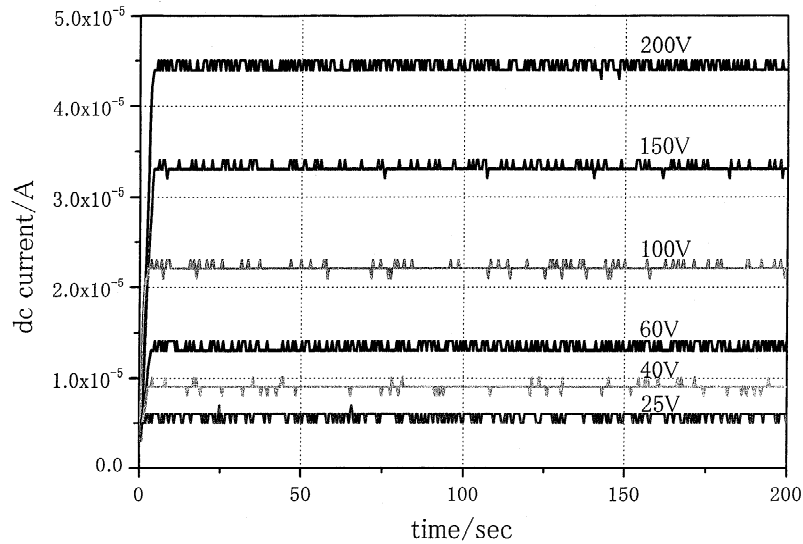


Fig. 2. Variation of the d.c. current with time through the  $\text{SrCe}_{0.95}\text{Yb}_{0.05}\text{O}_{3-\alpha}$  electrolyte under the various applied voltage. The steam electrolysis is made at  $150^\circ\text{C}$  and the partial pressure of water vapor is 355 Torr.

accumulated in the negative electrode by the steam electrolysis can be evaluated directly from the ERDA measurements [6].

Using the experimental apparatus described before [4,5], we evaluate the proton flux (protonic current) across the  $\text{SrCe}_{0.95}\text{Yb}_{0.05}\text{O}_{3-\alpha}$  electrolyte from both measurements of the d.c. current and the ERDA spectrum for the Zr electrode. Fig. 4 shows the number of hydrogen retained in the cathode against the operation time of the electrochemical cell. The slope of the fitted line in Fig. 4 may correspond to the proton flux. The proton flux increases with increasing temperature. Comparison between the proton flux and the d.c. current across the electrolyte reveals that the proton transport number is near unity above  $160^\circ\text{C}$  is consistent with the result obtained by the

EMF measurement [7]. This result shows that the migrating protons from the electrolyte were trapped in Zr metal with 100% efficiency.

From the proton flux  $\mathbf{J}$ , the diffusion coefficient of hydrogen  $\mathbf{D}$  could be determined by the following relation [8]

$$\mathbf{J} = cD\phi \text{ grad}/kT, \quad (1)$$

where  $\text{grad } \phi$  is the voltage drop per unit length of specimen,  $c$  is proton concentration and  $kT$  has usual meaning. The proton concentration determined by the ERDA measurements was 3.0 mol%, which was used in the present calculation.

Fig. 5 shows the Arrhenius plot of the diffusion coeffi-

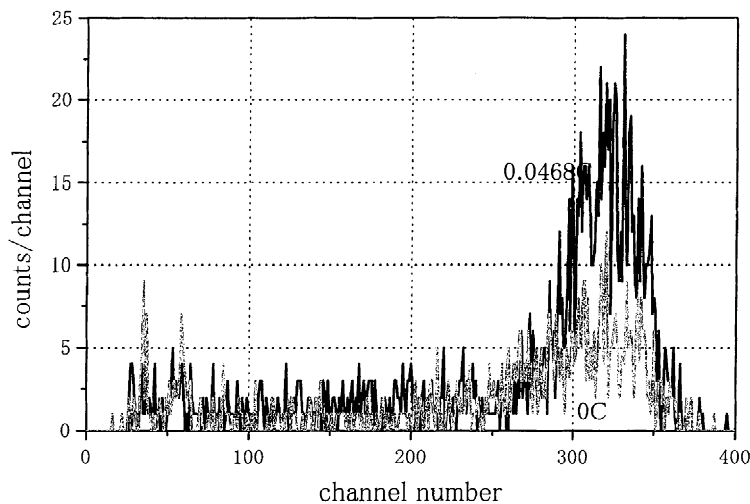


Fig. 3. ERDA spectra taken from the V electrode before and after the electrolysis at  $120^\circ\text{C}$ . The d.c. current across the electrolyte is 0.1 C.

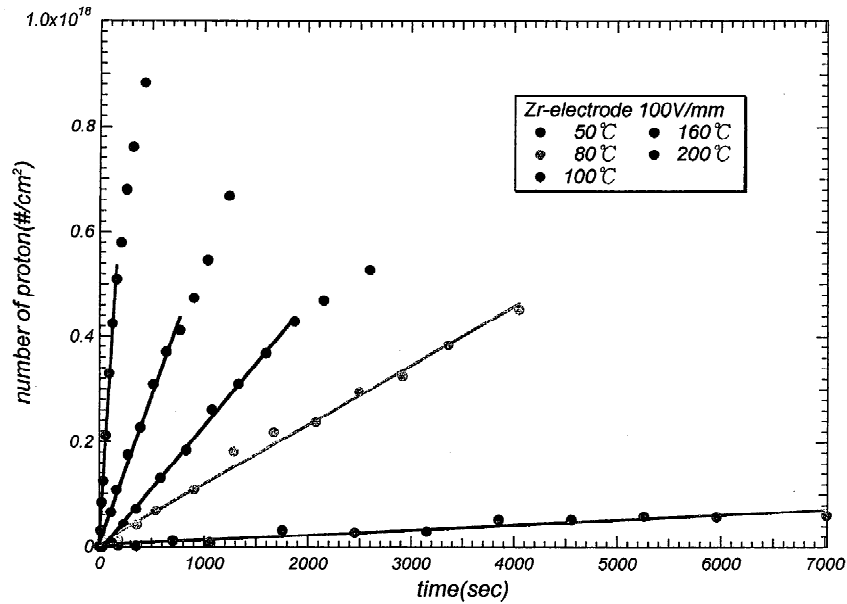


Fig. 4. Number of hydrogen in the negative electrode against time at various temperatures.

cient of proton in  $\text{SrCe}_{0.95}\text{Yb}_{0.05}\text{O}_{3-\alpha}$ . The proton diffusivities are of the order of  $10^{-12}$ – $10^{-10}$   $\text{cm}^2 \text{s}^{-1}$  in the temperature range of 50–200°C. Several diffusion or mobility data for protons in  $\text{SrCe}_{0.95}\text{Yb}_{0.05}\text{O}_{3-\alpha}$  has been reported [9–11]. The present results nearly agrees with the extrapolated value of the mobility data reported by Uchida et al. [9], but it is one order of magnitude smaller than the values reported by Matzke et al. [10]. The activation energy of about 0.50 eV is almost the same as the values reported by them.

The proton transport from the hydrogen storage metal to the proton conducting oxide is investigated by measurements of the open circuit voltage across the  $\text{SrCe}_{0.95}\text{Yb}_{0.05}\text{O}_{3-\alpha}$  oxide. The experimental routine consists of the following steps:

- (i) Hydrogen was charged in the negative electrode materials of V, Nb and  $\text{LaNi}_5$  by the gas-solid reaction or the steam electrolysis.
- (ii) The negative component of electrochemical cell was sealed tightly to prevent the leak of hydrogen gas. While the positive electrode was exposed to air. The cell temperature was adjusted in the range 50–500°C.
- (iii) A d.c. voltage of 25 V was applied to induce the proton migration. After disconnection the voltage the temporal evolution of the cell EMF was measured.

Fig. 6 shows the time evolution of the voltage for the electrochemical cell with the H-contained Nb metal as the negative electrode. The higher EMF voltage is observed at

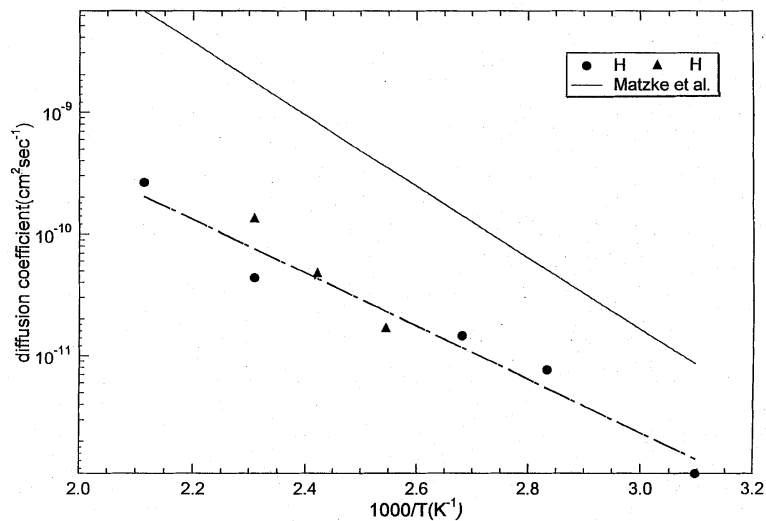


Fig. 5. Arrhenius plot of diffusion coefficient for proton in  $\text{SrCe}_{0.95}\text{Yb}_{0.05}\text{O}_{3-\alpha}$ .

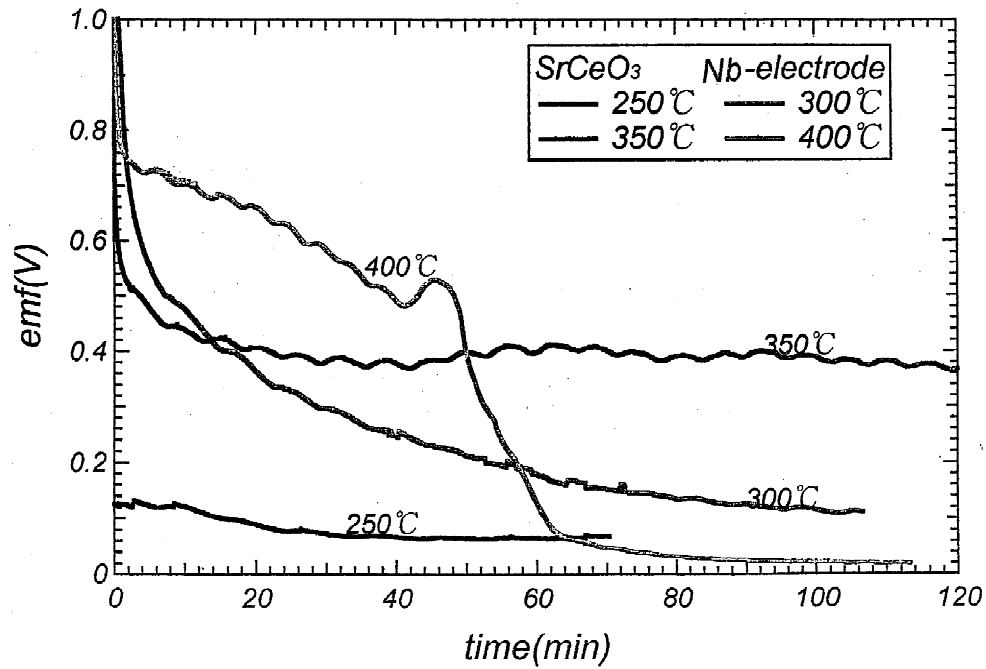


Fig. 6. EMF from the electrochemical cell consisting of  $\text{SrCe}_{0.95}\text{Yb}_{0.05}\text{O}_{3-\alpha}$  electrolyte and Nb negative electrode at various temperatures.

the higher temperature. This result is consistent with the performance of the hydrogen concentration cell reported by Iwahara et al. [12], where the cell EMF increases with increasing the cell temperature as well as the partial pressure of hydrogen in the negative component. The sudden drop of EMF observed at 400°C may be attributed to the drain of hydrogen from the Nb film.

The same experiment was made on the electrochemical

cell with Au electrodes from which the migration of hydrogen to the proton conducting oxide does not occur. Fig. 7 shows the time evolution of the voltage for the electrochemical cell where both Au electrodes are exposed to the same atmosphere. The EMF voltage caused by the concentration gradient of proton in the proton conducting oxide decreases with increasing temperature and also decreases gradually with time due to the decay of the

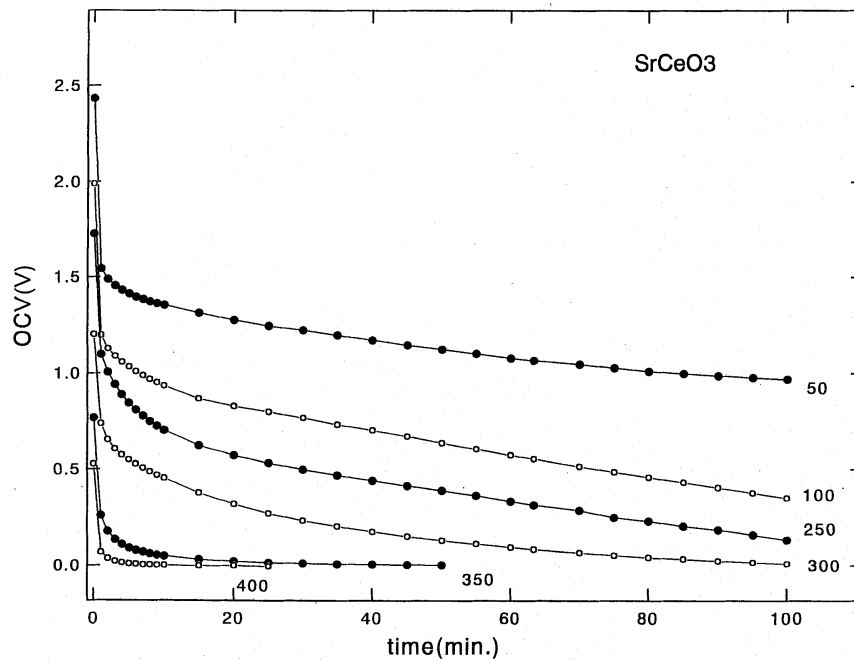


Fig. 7. EMF from the electrochemical cell consisting of  $\text{SrCe}_{0.95}\text{Yb}_{0.05}\text{O}_{3-\alpha}$  electrolyte and Au electrodes. Both electrodes are exposed to the same atmosphere.

concentration gradient in agreement with the result by Schober et al. [11]. The results described above provide the evidence that the hydrogen atom in the hydrogen storage metals move to the proton conducting oxide in the form of proton at high temperature. This result indicates that the hydrogen storage metals work as the negative hydrogen electrode of the hydrogen–air fuel cell.

#### 4. Summary

In an ERDA experiment we have measured the flux of protons migrating from the positive electrode to the negative electrode. Together with the result of electric current measurements, we determined proton transport numbers as well as diffusion coefficients of protons in  $\text{SrCe}_{0.95}\text{Yb}_{0.05}\text{O}_{3-\alpha}$  oxide at various temperatures. The EMF measurement provided the evidence that the hydrogen atoms in the hydrogen storage metal moved to the proton conducting oxide at high temperatures.

#### Acknowledgements

This work has been supported in part by a Grant-in-Aid for Scientific Research on Priority Areas (No. 299) from the Ministry of Education, Science, Sports and Culture.

#### References

- [1] H. Iwahara, *Solid State Ionics* 77 (1995) 289.
- [2] C. Folonari, G. Iemmi, F. Manfredi, A. Rolli, *J. Less-Common Met.* 74 (1980) 371.
- [3] E.W. Justi, H.H. Ewe, A.W. Kalberlak, N.M. Saridakis, M.H. Schaeffer, *Energy Conversion* 10 (1970) 183.
- [4] A. Kunimatsu, T. Arai, K. Takahiro, S. Nagata, S. Yamaguchi, Y. Akiyama, N. Sata, M. Ishigame, *Mat. Res. Soc. Symp. Proc.* 513 (1998) 209.
- [5] T. Arai, A. Kunimatsu, K. Takahiro, S. Nagata, S. Yamaguchi, Y. Akiyama, N. Sata and M. Ishigame, *Solid State Ionics* 121 (1999) 263.
- [6] J.C. Barbour, B.L. Doyle, *Handbook of Modern Ion Beam Material Analysis*, in: J.R. Tesmer, N. Nastasi (Eds.), M.R.S., Pittsburgh, 1995, p. 83.
- [7] A. Mitsui, M. Miyayama, H. Yanagida, *Solid State Ionics* 22 (1987) 213.
- [8] R.A. Oriani, O.D. Gonzalez, *Trans. Met. Soc. AIME* 239 (1967) 1041.
- [9] H. Uchida, H. Yoshikawa, T. Esaka, S. Ohtsu, H. Iwahara, *Solid State Ionics* 36 (1989) 89.
- [10] Th. Matzke, U. Stimming, Ch. Karmonik, M. Soetratmo, R. Hempelmann, F. Guthoff, *Solid State Ionics* 86–88 (1996) 621.
- [11] T. Schober, J. Friedrich, J.B. Condon, *Solid State Ionics* 77 (1995) 175.
- [12] H. Iwahara, H. Uchida, N. Maeda, *Solid State Ionics* 11 (1983) 109.